J. Membrane Biol. 106, 123–134 (1988)

The Journal of
Membrane Biology

Electrophysiological Properties of *Dictyostelium* Derived from Membrane Potential Measurements with Microelectrodes

Bert Van Duijn,†‡ Dirk L. Ypey,‡ and Loek G. Van der Molen†

†Cell Biology and Genetics Unit, Zoological Laboratory, University of Leiden, NL-2300 RA Leiden, The Netherlands, and
‡Department of Physiology and Physiological Physics, University of Leiden, NL-2333 AL Leiden, The Netherlands

Summary. Electrical membrane properties of the cellular slime mold *Dictyostelium discoideum* were investigated with the use of intracellular microelectrodes. The rapid potential transients (1 msec) upon microelectrode penetration of normal cells had a negative-going peak-shaped time course. This indicates that penetration of a cell with a microelectrode causes a rapid depolarization, which can just be recorded by the microelectrode itself. Therefore, the initial (negative) peak potential transient value E_p (−19 mV) should be used as an indicator of the resting membrane potential E_m of *D. discoideum* before impalement, rather than the subsequent semistationary depolarized value E_n (−5 mV). Using enlarged cells such as giant mutant cells (E_p = −39 mV) and electrofused normal cells (E_p = −30 mV) improved the reliability of E_p as an indicator of E_m. From the data we concluded that E_m of *D. discoideum* cells bathed in (mM) 40 NaCl, 5 KCl and 1 $CaCl_2$ is at least −50 mV. This potential was shown to be dependent on extracellular potassium. The average input resistance R_i of the impaled cells was 56 MΩ for normal *D. discoideum*. However, our analysis indicates that the membrane resistance of these cells before impalement is >1 GΩ. Specific membrane capacitance was 1–3 pF/cm^2. Long-term recording of the membrane potential showed the existence of a transient hyperpolarization following the rapid impalement transient. This hyperpolarization was associated with an increase in R_i of the impaled cell. It was followed by a depolarization, which was associated with a decrease in R_i. The depolarization time was dependent on the filling of the microelectrode. The present characterization of the electrical membrane properties of *Dictyostelium* cells is a first step in a membrane electrophysiological analysis of signal transduction in cellular slime molds.

Key Words membrane potential · *Dictyostelium discoideum* · microelectrode · peak transient · hyperpolarization · potassium conductance

Introduction

The cellular slime mold *Dictyostelium discoideum* provides a good model system for studying transmembrane signal transduction and the role of signal transduction in cellular differentiation. This simple organism has a two-stage life cycle, consisting of a unicellular vegetative stage and a multicellular aggregated stage. In the vegetative stage, *D. discoideum* is a free, in the soil, living amoeba feeding on bacteria. The multicellular stage develops by aggregation of the cells induced by exhaustion of the food supply. Aggregation is mediated by a chemoattractant, which is secreted by the cells and has been identified as cyclic AMP (cAMP) [17]. The multicellular aggregates form fruiting bodies producing spores.

During aggregation, cAMP acts as an extracellular hormone-like signaling agent and is detected by cell surface receptors. Binding of cAMP to the cAMP receptors induces a variety of intracellular responses, including a rapid but transient activation of adenylate cyclase and guanylate cyclase [8, 27]. Various experiments indicate a possible role for ions in the cAMP signal transduction. For example, the addition of cAMP to suspensions of *D. discoideum* results in changes in extracellular calcium- [5, 6, 20] and potassium-concentrations [1]. Potassium and calcium fluxes may reflect changes in membrane conductance and potential. Therefore, knowledge of the membrane potential of *D. discoideum* and its ionic mechanism is required to study the role of transmembrane ionic currents in transmembrane signal transduction. Furthermore, the interpretation of single ion channel measurements in these cells also requires knowledge of the membrane potential [22].

Given the extensive knowledge of biochemical mechanisms of signal transduction in *D. discoideum* developed in the last years [8, 27], the application of membrane electrophysiological techniques may provide new insights into the mechanism of signal transduction in *D. discoideum*. The availability of *D. discoideum* mutants with known defects in signal transduction may then be of great use in this approach. *Dictyostelium* cells can survive in rapidly changing ionic conditions, which indicates a power-

ful regulation of intracellular ion concentrations [21]. This regulation, probably by a combined action of ion pumps and ion channels, may also be expected to involve membrane potential control.

The patch-clamp technique in the whole-cell configuration cannot always be used to determine membrane potentials and membrane potential changes. On many cell types giga-seal formation is not yet possible. So far, no giga-seals on *Dictyostelium* cells bathed in normal saline solutions (i.e., solutions containing potassium and <1 mM Ca^{2+}) could be made [22; *unpublished observations*]. Enzyme treatment to facilitate giga-seal formation may damage the membrane. The exchange of the normal intracellular constituents of the cell and the clamping of artificial intracellular ion concentrations (especially calcium) in the whole-cell configuration are draw backs in the use of the patch-clamp technique in the study of the effect of drugs on the membrane potential.

Microelectrode measurements, when applied carefully, provide a method to directly measure the membrane potential of intact cells. Since microelectrode penetration induces a transmembrane shunt resistance, microelectrode measurements, especially in small cells, should be interpreted with care [13, 18]. This shunt resistance is probably located in the hydration mantle surrounding the microelectrode. Membrane potential measurements with microelectrodes in high-resistance cells usually suffer from sustained depolarization of the resting membrane potential due to the transmembrane shunt resistance [2, 13, 16, 24]. However, an analysis of the fast potential transient occurring within the first milliseconds after impalement may still provide information about the preimpalement electrical membrane properties of the cell [13]. Because *Dictyostelium* cells are relatively small (diameter $<$ 10 μm), a sustained depolarization of the membrane potential upon microelectrode impalement might be present.

In the present study, we report membrane potential measurements in *Dictyostelium* including an analysis of the fast potential transient upon microelectrode impalement. Enlargement of cells is introduced as a method to check the reliability of the peak potential transient as a measure of the true membrane potential. We evaluate the application of microelectrodes in these cells and give an estimation of the membrane potential, resistance and capacitance of *D. discoideum* cells bathed in a Na^+-saline solution. Our results are evidence that the potassium equilibrium potential as well as electrogenic ion pumps contribute to the membrane potential of *D. discoideum*.

The present study provides an electrophysiological basis for future research involving the role of ions and ion channels in transmembrane signal transduction of *D. discoideum*.

Materials and Methods

Cell Culture Conditions

Cells used for experiments included three types of *D. discoideum* cells.

First, *D. discoideum* NC4-H, which was grown together with *Escherichia coli* 281 on solid medium containing 3.3 g peptone, 3.3 g glucose, 4.5 g KH_2PO_4, 1.5 g $Na_2HPO_4 \cdot 2H_2O$, and 15 g agar per liter. After 40 hr incubation at 22°C, the cultures were harvested with cold 10 mM sodium/potassium phosphate buffer (pH 6.5). The cells were washed free of bacteria by three washes and by centrifugation at $150 \times g$ for 2 min. Subsequently, the cells were deposited on glass cover slips, with thickness of 0.17 mm (roughly 5×10^4 cells/cm^2), in petri dishes and stored for at least 2 hr, but not longer than 4 hr, at room temperature.

Second, electrofused *D. discoideum* cells were used [23]. After harvesting and washing, the cells were resuspended in 10 mM sodium/potassium phosphate buffer (10^8 cells/ml). Cell fusion was accomplished by four pulses of 5 kV/cm with 3-sec interval. Thereafter, the cell suspension was handled in the same way as the normal cells. The cell suspensions treated in this way contained, in addition to cells of normal size, some cells of remarkably increased size. The large cells from these suspensions were used for experiments.

Additionally, we used mutant *Dictyostelium* cells with disrupted myosine heavy-chain gene, called hmm-cells [7]. These cells exhibit relatively normal karyokinesis but limited cytokinesis, causing the formation of large cells. The cAMP-induced cAMP, cGMP and chemotactic responses in hmm-cells were not altered as compared with normal cells [26]. The hmm-cells were grown on plastic support in HL5-medium supplemented with 20 U/ml streptomycin/penicillin and 10 μg/ml G418 (Sigma Chemical Co.). The cells were harvested with growth medium and collected by centrifugation at $150 \times g$ for 2 min. Subsequently, the cells were resuspended in 10 mM sodium/potassium buffer and deposited on glass cover slips.

The membrane area of all the cells used was estimated by taking two times the area enclosed by the estimated cell circumference. Since these cells are rather flat, this appeared to be the best method to estimate the membrane area of cells adhered to the glass cover slip.

During experiments, the cells were bathed in a Na^+-saline solution composed of 40 mM NaCl, 5 mM KCl, 1 mM $CaCl_2$ and 1 mM HEPES-NaOH (pH 7.0). *D. discoideum* cells showed normal development when starved on solid medium containing Na^+-saline solution and 15 g agar per liter. The K^+-saline solution used consisted of 50 mM KCl, 5 mM NaCl, 1 mM $CaCl_2$ and 1 mM HEPES-KOH (pH 7.0). Furthermore, a Ca^{2+}-saline solution was used composed of 10 mM Ca(Cyclamate)$_2$, 10 mM $CaCl_2$ and 1 mM HEPES-KOH (pH 7.2).

Electrophysiology

For electrophysiological experiments, the glass cover slips with the adhered cells were mounted to an open-bottom Teflon culture dish, which placed on the stage of an inverted microscope permitted measurements using an objective magnification of 100× with oil immersion optics [14].

Membrane potential measurements were made with microelectrodes and a microelectrode amplifier with capacitance com-

Table. Membrane electrophysiological properties (mean values) of normal *D. discoideum* cells (DdH), electrofused *D. discoideum* cells (DdHfused) and giant mutant cells (hmm), bathed in Na^+-saline solution[a]

	E_p (mV)	E_n (mV)	t_n (msec)	Area (μm^2)	R_i (MΩ)	C_m (pF)	E_h (mV)	$T_{1/2}$ (sec)
DdH	−19.1	−4.7	0.09	88	56	6.1	−12.1	1.9
(SD,*n*)	(3.8, 32)	(1.6, 32)	(0.02, 32)	(52, 32)	(14, 10)	(0.8, 10)	(4.6, 24)	(1.4, 24)
DdHfused	−30.2	−6.0	0.13	790	33	—	−10.7	3.1
(SD,*n*)	(5.0, 36)	(2.0, 36)	(0.05, 36)	(410, 36)	(11, 26)		(4.7, 15)	(2.5, 15)
hmm	−38.9	−12.0	0.54	1724	35	12.2	−15.8	6.5
(SD,*n*)	(4.2, 127)	(2.0, 127)	(0.22, 127)	(181, 127)	(12, 29)	(3.9, 29)	(6.1, 45)	(4.9, 45)

[a] Given are: E_p, the peak value of the fast potential transient observed upon impalement as indicated in the text. E_n, the depolarized "steady-state" potential, which is reached just after E_p has appeared. t_n, the time to reach two-thirds of the depolarization to E_n after E_p was reached. Area, the estimated membrane area measured as indicated in the text. R_i, input resistance of the impaled cells just after the potential reached the value E_n. C_m, capacitance of the cell membrane determined as indicated in the text. E_h, the maximal hyperpolarized potential after E_n was reached. $T_{1/2}$, the time to reach one-half of the depolarized potential after E_h was reached.

All differences measured between the three cell types of the different electrophysiological properties are significant (Student's *t* test, 97.5% level) except for R_i of DdHfused and hmm cells, and E_h and $T_{1/2}$ of DdH and DdHfused cells.

pensation (WPI Series 700 Micro Probe Model 750, WP Instruments, New Haven, CT). Fine-tipped open-end microelectrodes with wide-angle tapers, filled with 3 M KCl had resistances of 83 MΩ (SD = 27 MΩ, n = 72) measured in Na^+-saline. Microelectrode capacitance was compensated avoiding overshoots in the potential response upon a current pulse applied to the microelectrode. The volume of the bathing solution in the dish was kept minimal during the measurements in order to reduce microelectrode capacitance. In this way, microelectrodes were obtained with rise times (= time to reach 66% of the potential response upon a current pulse) lower than 0.05 msec (range 0.05–0.02 msec). Electrode tip potentials were measured according to Blatt and Slayman [4] and ranged from 0 to −15 mV. All potential values have been measured with respect to the tip potential. A piezo-stepper device (Piezo-stepper P-2000, Physik Instrumente (PI) Gmbh Co., Waldbronn-Karlsruhe, F.R.G.) was used to ensure rapid (4 μm/0.1 msec), radial (at an angle of 60° from the horizontal) impalements of cells with minimal lateral vibration as opposed to impalement by hand. This device gives a minimal variation in the impalement-induced shunt resistances. The membrane-potential recordings were stored on FM magnetic tape (high frequency cut-off 20 kHz), and analyzed thereafter using a storage oscilloscope and a micro PDP-11 computer. Measurements were carried out at room temperature. Significance (95% level) of differences in results were tested with Student's *t* test.

Materials

The hmm-cells were a kind gift of Dr. J.A. Spudich, Department of Cell Biology, Stanford University School of Medicine. Chemicals were obtained from Sigma Chemical Co.

Results

Peak Potential Transients Upon Microelectrode Impalement

In our first experiments, we investigated the possibility to use intracellular microelectrodes to measure electric properties of normal *D. discoideum* cells such as membrane potential, resistance and capacitance. *Dictyostelium* cells are relatively small (diameter < 10 μm). Therefore, a peak-shaped potential transient is to be expected within the first milliseconds upon microelectrode penetration [13]. We used microelectrodes with sufficiently small rise times (<0.05 msec) to establish conditions under which fast transients could be measured. Upon touching the cell with the microelectrode a small (<4 mV) positive prepotential was seen.

Figure 1*A* shows a typical negative-going peak-shaped potential transient observed upon impalement of a *D. discoideum* cell with a microelectrode. The potential transient reaches a peak value E_p within 0.1 msec, which is followed by a depolarization of the membrane to a level E_n. In Na^+-saline, the mean values of E_p and E_n are −19.1 mV and −4.7 mV (*see* Table), respectively. The mean time of the potential to reach two-thirds of the depolarization to E_n after E_p was reached, t_n, was 0.09 msec (Table) in *D. discoideum* cells. The E_p value measured with 4 M potassium acetate (KAc) filled microelectrodes did not differ from those measured with 3 M KCl filled electrodes (4 M KAc: E_p = −21.0 mV (SD = 7.8 mV, n = 13)). The fact that this transient is observed already indicates that the measuring probe itself (the microelectrode) loads the potential measurement, as explained in Fig. 1*B*, with the use of an electrical circuit representation of the measurement condition.

From the two exponential potential responses (Fig. 1*C*) upon +150 pA current pulses applied to the microelectrode just after E_n was reached, we calculated the membrane resistance and capacitance. Because of the large difference between the microelectrode time constant and the time constant

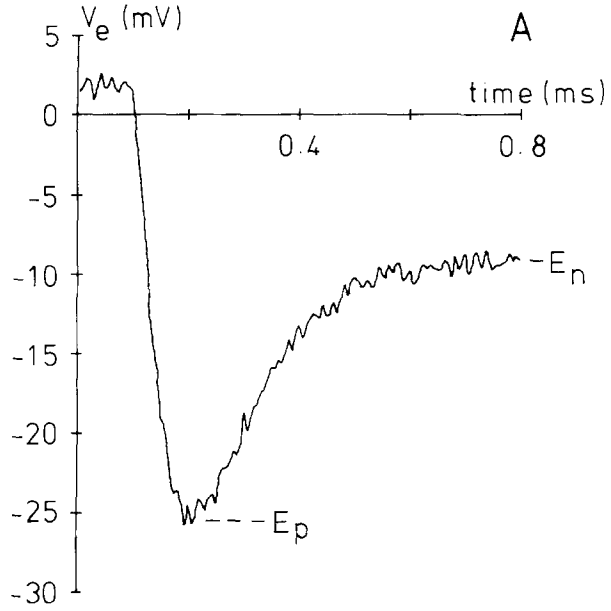

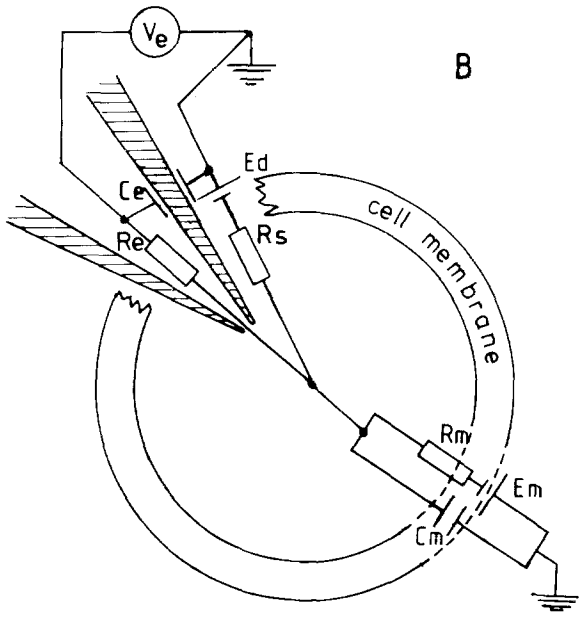

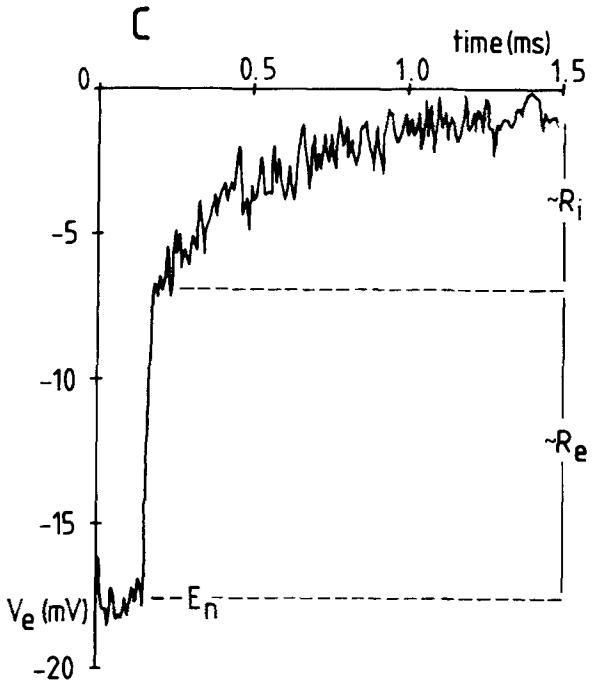

Fig. 1. (*A*) Peak-shaped potential transient recorded upon microelectrode penetration of a *D. discoideum* cell bathed in Na^+-saline solution. The initial positive deviation from the base line is the small prepotential seen upon touching the cell with the microelectrode. Rise time of the microelectrode was 0.03 msec. The microelectrode resistance was 84 MΩ. (*B*) Equivalent electrical circuit representation of a microelectrode measurement used in the analysis of peak-shaped potential transients. Microelectrode parameters are the microelectrode resistance R_e, and the microelectrode capacitance C_e. Cell parameters are the resting membrane potential E_m, the membrane resistance R_m, and the membrane capacitance C_m. Impalement of the cell by the microelectrode introduces a transmembrane shunt resistance R_s, associated with a diffusion potential E_d (cartoon design by C. Ince). (*C*) Two-component potential response to a current pulse of +150 pA applied to the microelectrode impaled into a *D. discoideum* cell and recorded just after E_n was reached. The component of the potential response due the microelectrode resistance and of that due to the impaled cell membrane are indicated by R_e and R_i, respectively. The cell was bathed in Na^+-saline solution. The microelectrode rise time was 0.025 msec, and the microelectrode resistance 71 MΩ. This cell showed a much more negative E_n as compared with most of the other *D. discoideum* cells

of the impaled cell membrane, these two time constants could be clearly distinguished. The time constant of the rapid phase was recognized as the microelectrode time constant. The time constant of the slow phase was that of the penetrated cell membrane. The mean membrane capacitance of *D. discoideum* cells was calculated to be 6.1 pF (Table). When divided by the estimated membrane area of these selected *D. discoideum* cells (220 μm^2, SD = 59 μm^2, $n = 10$), we find for the specific capacitance of the membrane of these cells 2.7 $\mu F/cm^2$ (SD = 0.4 $\mu F/cm^2$, $n = 10$). Furthermore, the input resistance (R_i) of the impaled cells was calculated from the same potential responses and was 56 MΩ (Table) in *D. discoideum*.

The difference between E_p and E_n indicates that the membrane resistance, R_m, is much larger than the microelectrode-induced shunt resistance, R_s [13]. Therefore, the value of R_i will be mainly determined by R_s. We conclude from these observations that the stable membrane potential E_n differs from the true membrane potential E_m, and that E_p is a

better estimate of E_m than E_n. However, E_p may still differ from the true resting membrane potential [13].

Theoretical Analysis

Peak transient measurements in combination with whole-cell membrane potential measurements in other types of cells showed that the peak transient can be a good estimate of the true membrane potential [13]. Whether the measured values of E_p in *D. discoideum* also are a fair approximation of the membrane potential may be expected to depend on the electrophysiological properties of these cells.

Mathematical analysis of a microelectrode penetration measurement with the use of an electrical circuit (Fig. 1*B*) has shown that the membrane resistance (R_m) has little effect on the value of E_p for $R_m > R_s$ [13] (*see also* Appendix). The membrane capacitance (C_m) and the microelectrode-induced shunt resistance (R_s), however, strongly affect the measured value of E_p [13]. This indicates an important role for the membrane area in the accuracy of the peak transient measurements.

To demonstrate the usefulness of cells with increased membrane area in the analysis of peak transient measurements, we used the equivalent electrical circuit (*cf.* Fig. 1*B*) described by Ince et al. [13].

When a microelectrode enters a cell, the impaled tip is no longer exposed to the bathing solution, so the microelectrode capacity with respect to ground may slightly decrease upon impalement. We neglected this change since the dividing of the microelectrode capacitance, C_e, in a major component outside the cell and minor component (up to 25% of total C_e) inside the cell upon impalement did not alter the number of exponents required to describe the circuit. In addition, the effect of this procedure on the value of E_p was negligible (<0.17%, data not shown).

We calculated the value of the E_p to E_m ratio (E_p/E_m) as a function of C_m. R_e and C_e values were taken from microelectrode measurements in normal *D. discoideum* cells. For R_s, the input resistance of the impaled cell measured during E_n, just after the peak transient was chosen. This is valid when $R_m \gg R_s$. The difference between E_p and E_n indicates that this is true for the cells used. The diffusion potential, E_d, across the microelectrode-induced shunt resistance was supposed to be zero.

Figure 2 shows the exponential relationship between E_p/E_m and C_m for a constant R_m. Increasing the membrane capacitance increases the value of E_p/E_m. We did calculations with a nonvarying cell membrane time constant (R_mC_m), obtained by decreasing R_m with increasing C_m. Variation of R_m

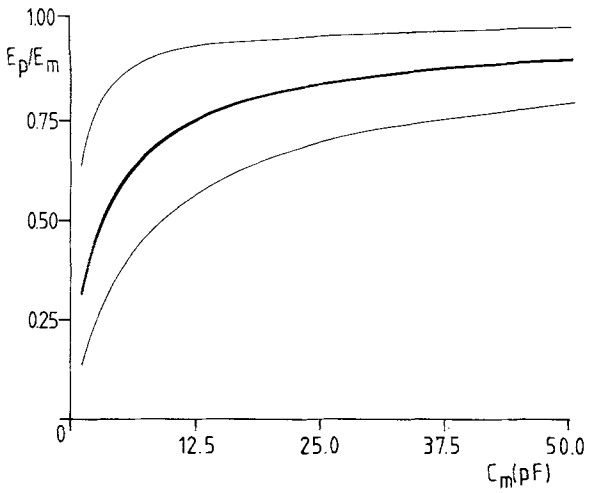

Fig. 2. E_p to E_m ratio as a function of C_m as calculated with the use of the equivalent electrical circuit (Fig. 1*B*). The values of the circuit parameters used here are: R_m = 2 GΩ, R_e = 83 MΩ (27), R_s = 56 MΩ (14), C_e = 0.8 pF (0.6), E_m = −100 mV, and E_d = 0 mV (SD between parentheses). Upper curve shows the relationship for the most favorable conditions for E_p as a good indicator of E_m. Middle curve for the mean conditions and the lower curve for the worst conditions

between 2 GΩ and 40 MΩ only gave a maximal deviation in E_p's of −2.7% from the values calculated with a constant R_m of 2 GΩ (*data not shown*). Calculations with E_d = −5 mV, which is the most negative value E_d can be since the mean E_n is −5 mV in these cells, did not show different E_p values within +3.2% as compared with the conditions used for analysis (*data not shown*). Figure 2 shows that the value of E_p will approach E_m closely when C_m is large enough. And because R_m only weakly influences the value of E_p, this also applies to cell size. Hence, increasing the cell size is a method to improve the reliability of E_p as an indicator of E_m. Alternatively, E_p may be considered as a good indicator of E_m if a further increase in cell size does not increase the value of E_p anymore.

Peak Potential Transients in Enlarged Cells

In other studies, X-irradiation-derived giant murine macrophage and fibroblast cell lines did not show different values of E_p as compared with normal cells, indicating E_p to be a good estimate of the true membrane potential in these cells [12].

To find out the relation between cell size and E_p in *D. discoideum*, we used two types of enlarged *Dictyostelium* cells.

First, electrofusion [23] was used to obtain large cells. The mean membrane area of the fused cells selected in our experiments was 790 μm^2 (Ta-

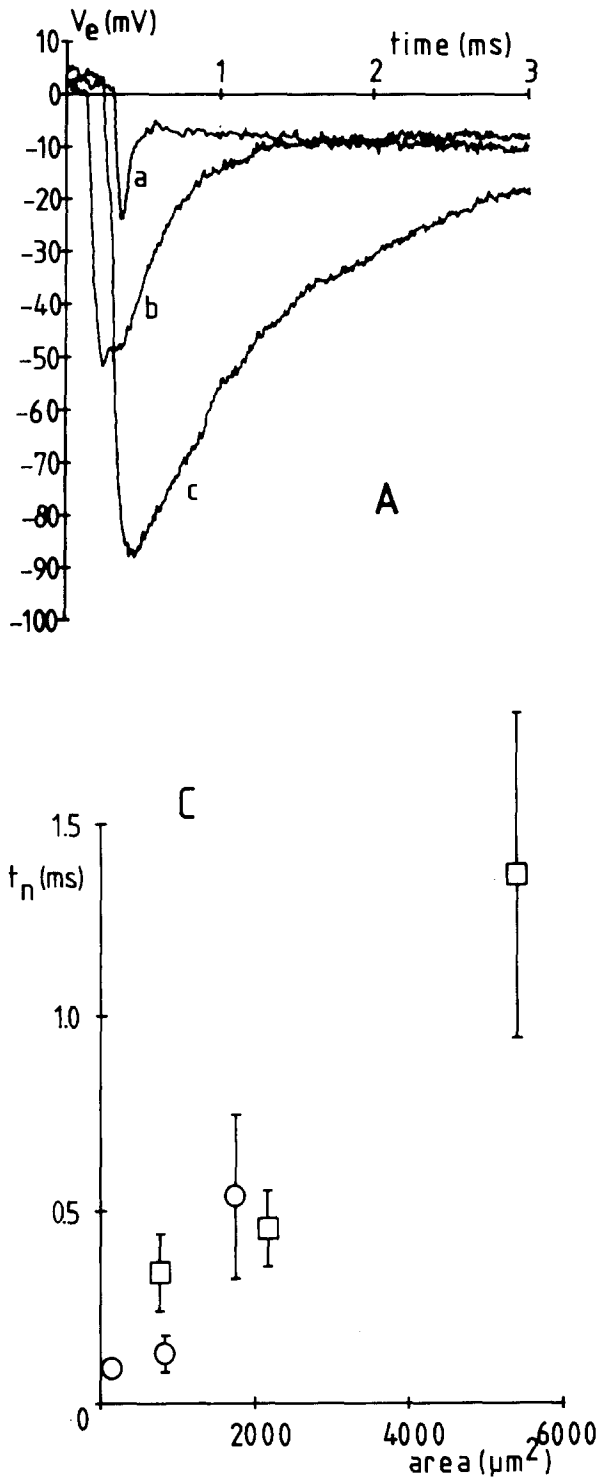

Fig. 3. (*A*) Peak potential transients measured in an electrofused *D. discoideum* cell (*b*), and a hmm-cell (*c*) bathed in Na^+-saline solution. For comparison the peak potential transient from Fig. 1*A* from a normal *D. discoideum* cell (*a*) is also shown. Both the increase in E_p and t_n with increasing cell size are apparent. (*B*) Peak potential transient properties as a function of the estimated cell membrane area of normal, electrofused and hmm *D. discoideum* cells. E_p (filled symbols) and E_n (open symbols) as a function of the estimated cell membrane area of normal (circles), electrofused (circles) and hmm-cells (circles). For the standard deviations of the estimated membrane areas see the Table. The squares show E_p (filled symbols) and E_n (open symbols) for hmm-cells of different size only. The estimated cell membrane areas of these cells are: 752 μm^2 (SD = 147 μm^2, $n = 66$), 2144 μm^2 (SD = 266 μm^2, $n = 49$), and 5360 μm^2 (SD = 1361 μm^2, $n = 12$). Bars indicate ± SD; no bar means SD < 2 mV. (*C*) Mean time of the potential decay to reach two-thirds of the depolarization to E_n after E_p was reached, t_n, as a function of the estimated cell membrane area. The same cells and symbols as in (*B*). Bars indicate ± SD

ble). This is about 10 times larger than that of normal cells. Figure 3*A* compares the negative-going peak-shaped potential transient of the three cell types used. One of these (curve *b*) is a potential transient observed upon impalement of an electrofused *D. discoideum* cell. Both E_p (−30.2 mV) and E_n (−6.0 mV) are more negative in electrofused cells bathed in Na^+-saline solution as compared with normal cells (Table).

The mean value of t_n in these cells was 0.13 msec (Table). The value of R_i, as measured directly after the membrane potential reached the value of

E_n, was 33 MΩ (Table) in electrofused cells. The slight difference in R_i between fused and normal cells indicates that R_s dominates over R_m.

Second, *D. discoideum* transformant hmm with giant cells was used. The mean membrane area of these cells selected for experiments was 1724 μm^2 (Table), about 20 times larger than in normal cells. In Figure 3*A* (curve *c*) a negative-going peak-shaped potential transient observed upon impalement of a hmm-cell is shown. Membrane potentials measured in hmm-cells in Na^+-saline were: E_p = −38.9 mV and E_n = −12.0 mV (Table). The values of t_n, C_m and R_i were determined. The value for t_n was found to be 0.54 msec (Table). The values of C_m and R_i were 12.2 pF (Table), and 35 MΩ, respectively (Table). The specific capacitance of the membrane of hmm-cells was estimated to be 1.3 $\mu F/cm^2$ (SD = 0.7 $\mu F/cm^2$, n = 29) by dividing C_m by the membrane area of the cells used in these experiments (mean 1169 μm^2 (SD = 572 μm^2, n = 29)). The measurements in hmm-cells show an increased value of E_p, E_n and t_n as compared with normal and electrofused cells, showing a relation between cell size and E_p, as expected.

Figure 3*B* shows measured E_p values as a function of the cell membrane area of the different cells used, suggesting a behavior of the measured E_p values as described by the equivalent electrical circuit calculations (Fig. 2). To indicate that these differences in mean E_p measured in the three cell types are only due to variations in membrane capacitance and not due to the different origins of these cells, Fig. 3*B* also shows E_p as a function of membrane area of hmm-cells. The dependence of E_p on the membrane area of the hmm-cells indicates that variation in membrane area for one cell type also leads to variation in the E_p measured, assuming that the true membrane potential does not depend on the cell size. This is evidence that the measured peak transient values in normal *D. discoideum* cells are not near to the true membrane potential. However, the E_p values measured in enlarged cells are closer to true membrane potential of *D. discoideum*.

Figure 3*C* shows the relationship between t_n and the cell membrane area for the same cells as in Fig. 3*B*. From the model, it is expected that t_n will be mainly determined by R_iC_m [13]. R_iC_m is proportional to the membrane area for cells with $R_m > R_s$. Therefore, the linear relationship between t_n and the membrane area shown in Fig. 3*C* is as expected for *D. discoideum* cells.

The Shunted Membrane Potential

In contrast with E_p, the value of E_n does not depend on C_m but on R_m. E_n follows from the relationship between membrane resistance, microelectrode-induced shunt resistance, membrane potential and diffusion potential of the shunt [13],

$$E_n = (E_mR_s + E_dR_m)/(R_m + R_s). \quad (1)$$

From Eq. (1), it follows that the smaller R_m (i.e., the larger the cells) the more E_n approaches the value of E_m. Figure 3*B* shows the values of E_n for the different cell types as a function of the membrane area. As expected from Eq. (1), the value of E_n is more negative for larger cells, consistent with the lower membrane resistance they have. Figure 3*B* also shows that E_p is always closer to the true membrane potential than E_n. Furthermore, this figure reveals that a much stronger enlargement of cells is required for E_n than for E_p to approach E_m.

Estimation of the True Resting Membrane Potential

Although the microelectrode measurements in *Dictyostelium* suffer from a loading shunt resistance, an estimation of the true resting membrane potential can still be made. Simulation of the rapid potential transients upon microelectrode impalement (Fig. 2) using parameter values as found in our experiments indicates a value for E_p/E_m of 0.39 for impalements of normal *D. discoideum* cells. This suggests that E_m is much more negative than the measured value of E_p. The measurements in the larger cells (Fig. 3*A* and *B*) support this evidence. We made an estimation of E_m from the E_p/E_m values (Fig. 2) for normal, fused and hmm-cells using the membrane capacitance of the different cell types (Table). In this way we find for normal *D. discoideum* cells, E_m = −50 mV (range −30 to −110 mV), for electrofused cells, E_m = −46 mV (range −33 to −66 mV) and for hmm-cells, E_m = −50 mV (range −40 to −65 mV). This method for making an approximation of the true membrane potential is rather unsatisfactory, since the range of these estimations is large, especially for the normal cells.

Another way to obtain an approximate value of E_m is extrapolation of the E_p data in Fig. 3*B*. Single exponential fitting of the E_p data points (according to Fig. 2) indicates that the membrane potential of *Dictyostelium* cells (i.e., the E_p value for extreme large membrane area) is −67 ± 13 mV (fitting with Gauss-Newton method, correlation coefficient = 0.98).

Occasionally in hmm-cells, E_p values around −80 mV were measured (mean of 10 largest E_p values measured = −82 mV, SD = 8 mV). This suggests that the membrane potential of these cells can

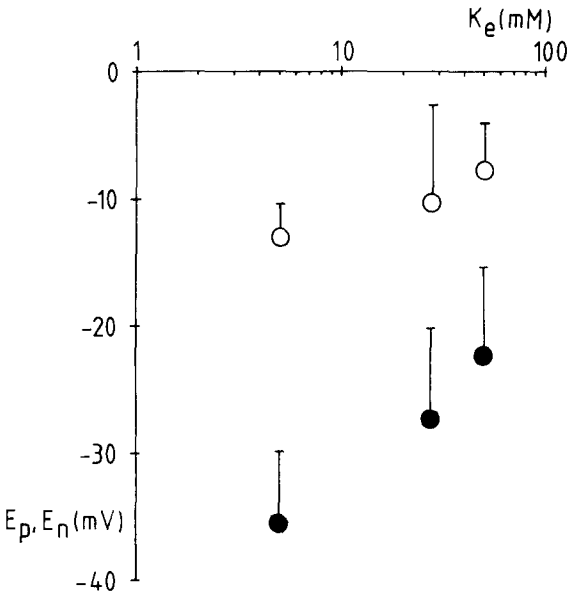

Fig. 4. E_p (filled symbols) and E_n (open symbols) as a function of the extracellular potassium concentration, K_e, in the bath. E_p and E_n were measured in hmm-cells with an estimated cell membrane area of 1275 μm^2 (SD = 308 μm^2, n = 96). Bars indicate + SD; n = 32 for each concentration

be at least −80 mV in Na^+-saline solution, which is in agreement with the data from Fig. 3*B*.

Different Ionic Conditions

The dependence of the membrane potential of *Dictyostelium* on different ionic conditions was investigated in order to explore the ionic mechanism of the membrane potential.

Changing the Na^+-saline solution for the K^+-saline solution or for a mixture of these solutions resulted in changed membrane potentials. These changes were measured within 15 min after the solution change. Figure 4 shows E_p and E_n for different extracellular K^+ concentrations for hmm-cells. Hmm-cells were used because potential changes could be measured more reliably in these cells (*see above*). However, normal *D. discoideum* cells also showed a less negative E_p in K^+-saline solution: E_p = −14.7 mV (SD = 4.5 mV, n = 19). In control measurements in Na^+-saline solution we found: E_p = −19.2 mV (SD = 4.3 mV, n = 15) (significant at 95% level).

Figure 4 shows that E_p is dependent on the extracellular K^+ concentration, which implies that the membrane potential of *D. discoideum* is dependent on extracellular potassium.

As expected, E_n only shows a weak dependency on the extracellular potassium concentration, because E_n is a bad indicator of the true membrane potential.

E_p measured in cells bathed for more than 30 min in K^+-saline solution were more negative than just after exchanging the Na^+-saline solution for the K^+-saline solution. This indicates that the membrane potential recovers from the initial depolarization. The action of electrogenic ion pumps and/or active ion transport might play a role in this recovery.

Patch-clamp measurements in the cell-attached patch mode have been done by others on *D. discoideum* cells bathed in calcium-saline solutions [22]. In order to provide membrane potential estimates for this type of experiments, we did membrane potential measurements on hmm-cells bathed in Ca^{2+}-saline solution. Membrane potentials under these conditions were: E_p = −32.7 mV (SD = 12.6 mV, n = 10), and E_n = −12.8 mV (SD = 10.9 mV, n = 10). Control measurements in Na^+-saline solution (with 1 mM $CaCl_2$) resulted in E_p = −31.8 mV (SD = 13.0 mV, n = 19), and E_n = −13.0 mV (SD = 4.3 mV, n = 19). Thus, there is no difference in membrane potential between cells bathed in Ca^{2+}-saline solution and in Na^+-saline solution (significant at 95% level).

Microelectrode-Induced Hyperpolarizing Response

Though the electrophysiological conditions of the *D. discoideum* cells change upon impalement, it is still of interest to study the membrane properties of the impaled cell. Certain ionic conductances may be expressed due to the damage [12, 28], or may still be measurable in spite of the microelectrode-induced shunt resistance.

After reaching E_n, the membrane potential in many cases (>60%) hyperpolarizes to a maximal negative potential E_h (Fig. 5). This hyperpolarization is accompanied by an increase in transmembrane resistance, which likely reflects an increase in the microelectrode-induced shunt resistance by a sealing of the membrane around the microelectrode [4]. When the E_h value is reached, the membrane slowly depolarizes again, with a half time of depolarization, $T_{1/2}$, to a sustained steady-state potential. The depolarization is accompanied by a decrease in transmembrane resistance (Fig. 5).

The E_h and $T_{1/2}$ values for normal *D. discoideum*, fused cells and hmm-cells bathed in Na^+-saline solution are given in the table. From these measurements it is clear that the E_h values are less negative than the E_p values measured in the same cells (Table). In addition, E_h is not strongly dependent on the cell size, in contrast with the value of E_p

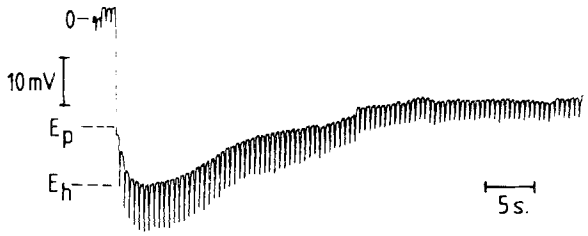

Fig. 5. Slow membrane potential changes upon microelectrode impalement into a *D. discoideum* cell bathed in Ca^{2+}-saline solution. Upon touching of the cell a small positive prepotential is seen. The initial rapid impalement peak potential transient, indicated by E_p, cannot be seen in this record because of the low high-frequency cut-off properties of the chart recorder used. Current pulses of −26 pA were applied to the microelectrode to monitor the input resistance, R_i. Microelectrode resistance was 107 MΩ

(Fig. 3*B*). However, the half time of depolarization, $T_{1/2}$, increases with increasing cell size.

In 4 hmm-cells (out of 49), a stable potential of −21.8 mV (range −14.4 to −29.6 mV) could be maintained for about three min. The corresponding E_p values of these four cells were much more negative than the stable potential values (E_p = −54.2 mV, range −24.8 to −91.9 mV).

Dictyostelium cells bathed in Ca^{2+}-saline solution showed a more negative hyperpolarization, E_h = −19.0 mV (SD = 2.0 mV, n = 45), as compared with cells bathed in Na^+-saline solution (significant at 95% level). However, $T_{1/2}$ was not increased in Ca^{2+}-saline solution ($T_{1/2}$ = 1.4 sec, SD = 0.2 sec, n = 45) (significant at 95% level).

In all experiments there was no correlation between the value of E_h and the value of $T_{1/2}$.

The increase of $T_{1/2}$ with increasing cell size indicates a possible role in the depolarization for the leakage of ions from the microelectrode into the cell. In order to find out whether this depolarization in *Dictyostelium* cells is caused by the leakage of chloride ions from the microelectrode into the cell as is the case in *Neurospora* cells [4] we did some additional experiments with different microelectrode fillings, in which Cl^- was lacking or strongly reduced.

We did measurements with 4 M KAc-filled microelectrodes on normal *Dictyostelium* cells bathed in Ca^{2+}-saline solution and on hmm-cells bathed in Na^+-saline solution. The value of E_h in the normal cells was −17.0 mV (SD = 2.0 mV, n = 14), and of $T_{1/2}$ was 1.7 sec (SD = 0.5 sec, n = 14). No hyperpolarized potentials stable at E_h were observed in these cells with the use of 4 M KAc-filled microelectrodes. In the hmm-cells, E_h was −12.6 mV (SD = 6.7 mV, n = 11), which is not different from E_h measured with 3 M KCl-filled microelectrodes (significant at 95% level). $T_{1/2}$ ranged from 4 sec to 3 min (mean 64 sec) when 4 M KAc-filled microelectrodes were used on hmm-cells. Nevertheless, stable potentials around or more negative than E_p were neither obtained on hmm-cells with the use of 4 M KAc-filled microelectrodes. Measurements with 0.1 M KCl-filled microelectrodes on normal *D. discoideum* cells bathed in Ca^{2+}-saline solution neither showed stable potentials around the E_p nor at the E_h value. Instead, a large variation in both E_h and $T_{1/2}$ was found. The mean E_h was −34.2 mV (SD = 30.1 mV, n = 10) and the mean $T_{1/2}$ was 30 sec (range 5 sec to 3 min, n = 10).

Discussion

The present study shows that microelectrode measurements in *D. discoideum* cells, when applied properly, can provide information about the electrical membrane properties of these cells. This has also been shown for various other high-resistance cell types [2, 13, 16, 18, 24]. The appearance of a rapid peak-shaped potential transient (Figs. 1*A* and 3*A*) upon microelectrode impalement of a *D. discoideum* cell shows the presence of a microelectrode-induced shunt resistance, which causes a sustained depolarization of the membrane potential. However, our results show that the peak transient value E_p of the rapid impalement transient is still the best available estimate for the true resting membrane potential of *D. discoideum*.

From the shape of the potential decay after E_p is reached (Figs. 1*A* and 3*A*) we conclude that changes in the microelectrode-induced shunt resistance during the potential transient are not significant in disturbing our measurements. The sealing of the membrane around the microelectrode, associated with an increase in shunt resistance, appears to occur on a larger time scale (*see* microelectrode-induced hyperpolarizing response and [4]).

Measurements in enlarged cells proved to be a good method to test the reliability of E_p as a measure of E_m. From the dependence of the measured peak transient potential on the cell size between the different cell types used (normal, fused and hmm) as well as within one cell type (Fig. 3*A* and *B*) we conclude that the true membrane potential of these different cell types is the same (assumed that E_m is cell size independent). An estimation of the true membrane potential was made from the simulations, from the dependence of E_p on the cell size and the occasionally appearing larger E_p values in hmm-cells. From these data, E_m was approximated to be at least −50 mV in Na^+-saline solution for all the cell types used. The measurements in hmm-cells indicate that E_m likely lies around −80 mV for *D. discoideum* cells in Na^+-saline solution. Measure-

ments of the intracellular sodium (minimal about 5 mM) and potassium concentrations (maximal about 50 mM) of *D. discoideum* have been done by others [1, 19, 21]. The Nernst potential for K^+ and Na^+ in cells bathed in Na^+-saline solution are −60 mV and +55 mV, respectively. The change of the peak transient upon changing of the external potassium concentration (Fig. 4) indicates that the membrane potential is dependent on selective potassium conduction. This dependency on the external K^+ concentration suggests the presence of a K^+ conductance, which could be due to K^+ channel activity in these cells [22]. A membrane potential of −90 mV in the true slime mold *Physarum polycephalum* was found by Hato and coworkers [10] with microelectrodes. In *Amoeba proteus* a membrane potential of −72 mV was reported, which is dependent on the extracellular K^+ concentration [3]. The estimation of the true membrane potential of *D. discoideum* and peak transients, which have been measured in hmm-cells, show that the true membrane potential is more negative than the Nernst potential for potassium for both Na^+- and K^+-saline solution. From this we conclude that electrogenic ion pumps also contribute to the membrane potential of *D. discoideum*. Experiments using ion pump blocking agents and different ion solutions are required to determine the contribution and nature of such factors to the membrane potential.

The shunted membrane potential, E_n, is less negative than E_p. Hence, R_m is large if compared with the microelectrode-induced shunt resistance. For larger cells, the value of E_n is more negative than for normal cells, which shows that the membrane resistance, R_m, becomes smaller with increasing cell size.

Since E_n follows from the relationship between R_m, R_s, E_m and E_d, Eq. (1), an estimation of R_m can be made. For $E_d = 0$, Eq. (1) reduces to:

$$E_n/E_m = R_s/(R_m + R_s) = R_i/R_m. \quad (2)$$

Therefore, with the estimated value of E_m, and the measured values of E_n and R_i, a minimum value for R_m can be calculated using Eq. (2). For normal *D. discoideum* cells, we find in this way for R_m at least 1 GΩ. For fused and hmm-cells we find 440 and 230 MΩ, respectively. Since R_i is much smaller than R_m, the measured input resistance of the impaled cells will be dominated by R_s.

The calculation of the specific membrane capacitance of *Dictyostelium* revealed a value between 1 and 3 $\mu F/cm^2$ for normal and hmm-cells. This outcome, together with the linear relationship found between t_n and the estimated cell membrane area, shows that the estimations of the membrane areas of these cells are of the right order of magnitude, as a value around 1 $\mu F/cm^2$ is commonly found for the specific capacitance of biological membranes [11].

A more negative membrane potential is expected in cells bathed in Ca^{2+}-saline solution, since this solution does not contain potassium, as compared with cells bathed in Na^+-saline solution. Our measurements show that no difference in membrane potential is present between cells bathed in Na^+-saline and Ca^{2+}-saline solution. This might be due to blockage of potassium-dependent electrogenic ion pumps by low extracellular potassium concentrations [9], which depolarizes the membrane.

The slow hyperpolarization followed by a depolarization occurring after the microelectrode-induced peak potential transient shows that, even in high-resistance cells, microelectrodes can be used to measure certain changes in electrophysiological properties while the cells are impaled.

In various cells, transient hyperpolarizations upon microelectrode penetration have been reported [4, 10, 12, 15, 25, 28]. These measurements, however, show microelectrode-induced hyperpolarizations accompanied by a decrease in transmembrane resistance, except for *Neurospora* cells [4]. In *Neurospora* cells, the hyperpolarization is accompanied by an increase in transmembrane resistance and is caused by a sealing of the cell membrane around the microelectrode. This sealing makes R_s larger so that the measured potential will be closer to E_m (*see* Eq. (1)). In addition, electrogenic ion pump currents will generate a larger potential when the input resistance of the cell increases.

The E_p values measured in Na^+-saline solution and Ca^{2+}-saline solution are not different. Therefore, the larger E_h values found in cells bathed in Ca^{2+}-saline solution as compared with cells bathed in Na^+-saline solution might be due to a better sealing of the membrane around the microelectrode for higher calcium concentrations. Because no correlation is present between E_h and $T_{1/2}$, the magnitude of the microelectrode-induced shunt resistance R_s, which determines the value of E_h reached, has no influence on the rate of depolarization. Hence, leakage through R_s of ions from the bath solution into the cell likely does not play an essential role in the depolarization of the measured potential after E_h is reached.

The increase of the half time of depolarization, $T_{1/2}$, with increasing cell size and the increase of $T_{1/2}$ when 0.1 M KCl-filled microelectrodes are used suggests that the depolarization is caused by leakage of ions from the microelectrode into the cell as is the

case with leakage of chloride ions from the microelectrode in *Neurospora* cells [4]. On the other hand, the experiments with 4 M KAc-filled microelectrodes do not confirm a role for leakage of chloride ions into the cell.

Although the value of E_h and $T_{1/2}$ could be changed with the use of different microelectrode fillings, we have not been able to record stable potentials with values around or more negative than the measured values of E_p. Therefore, the peak value E_p of the initial rapid impalement transient remains to be the best estimate of the membrane potential of *D. discoideum* cells. We conclude that leakage of ions from the microelectrode plays a role in the slow depolarization of the membrane potential after E_h. However, other processes (*e.g.*, changes in the sealing of the membrane around the microelectrode), which prevent the recording of stable potentials, will be present as well and need further investigation.

The present study shows that useful information about electrophysiological properties can be obtained by careful application of the microelectrode technique, even in small, high-resistance cells like *D. discoideum*. Our results concern the membrane potential, resistance and capacitance of non-stimulated *D. discoideum* cells. We consider these results as a basis for future research into the role of transmembrane currents and potentials in the response of *D. discoideum* to chemoattractants.

The authors wish to thank Dr. Ir. Can Ince, Dr. Peter J.M. Van Haastert, Henk P. Buisman, Johan E. Pinas, Prof. Dr. A.A. Verveen and Prof. Dr. T.M. Konijn for advice, support and stimulating discussions. We are very grateful to Kees Donkersloot for the design and the construction of the cell fusion instrument and Jan Van Hartevelt for computer assistance. We acknowledge the Foundation for Medical Research (MEDIGON) of the Netherlands and the Department of Infectious Diseases (Prof. Dr. R. van Furth) for the use of computer equipment for data processing.

References

1. Aeckerle, S., Wurster, B., Malchow, D. 1985. Oscillations and cyclic AMP-induced changes of the K^+ concentration in *Dictyostelium discoideum*. *EMBO* J. **4**:39–43
2. Bakker, R., Dobbelmann, J., Borst-Pauwels, G.W.F.H. 1986. Membrane potential in the yeast *Endomyces magnusii* measured by microelectrodes and TPP^+ distribution. *Biochim. Biophys. Acta* **861**:205–209
3. Bingley, M.S., Thompson, C.M. 1962. Bioelectric potentials in relation to movement in Amoebae. *J. Theor. Biol.* **2**:16–32
4. Blatt, M.R., Slayman, C. L. 1983. KCl leakage from microelectrodes and its impact on the membrane parameters of a nonexcitable cell. *J. Membrane Biol.* **72**:223–234
5. Bumann, J., Malchow, D., Wurster, B. 1986. Oscillations of Ca^{2+} concentration during the cell differentiation of *Dictyostelium discoideum*. *Differentiation* **31**:85–91
6. Bumann, J., Wurster, B., Malchow, D. 1984. Attractant-induced changes and oscillations of the extracellular Ca^{2+} concentration in suspensions of differentiating *Dictyostelium* cells. *J. Cell Biol.* **98**:173–178
7. De Lozanne, A., Spudich, J.A. 1987. Disruption of the *Dictyostelium* myosin heavy chain gene by homologous recombination. *Science* **236**:1086–1091
8. Devreotes, P.N. 1983. Cyclic nucleotides and cell-cell communication in *Dictyostelium discoideum*. *Adv. Cycl. Nucleotide Res.* **15**:55–96
9. Gorman, A.L.F., Marmor, M.F. 1970. Temperature dependence of the sodium-potassium permeability ratio of molluscan neuron. *J. Physiol. (London)* **210**:919–931
10. Hato, M., Ueda, T., Kurihara, K., Kobatake, Y. 1976. Changes in zeta potential and membrane potential of the slime mold *Physarum polycephalum* in response to chemical stimuli. *Biochim. Biophys. Acta* **426**:73–80
11. Hille, B. 1984. Ionic Channels of Excitable Membranes. Sinauer Associates, Sunderland, Massachusetts
12. Ince, C., Leijh, P.C.J., Meijer, J., Van Bavel, E., Ypey, D.L. 1984. Oscillatory hyperpolarizations and resting membrane potentials of mouse fibroblast and macrophage cell lines. *J. Physiol. (London)* **352**:625–635
13. Ince, C., Van Bavel, E., Van Duijn, B., Donkersloot, K., Coremans, A., Ypey, D.L., Verveen, A.A. 1986. Intracellular microelectrode measurements in small cells evaluated with the patch clamp technique. *Biophys. J.* **50**:1203–1209
14. Ince, C., Van Dissel, J.T., Diesselhoff, M.M.C. 1985. A Teflon culture dish for high-magnification microscopy and measurements in single cells. *Pfluegers Arch.* **403**:240–244
15. Ince, C., Van Duijn, B., Ypey, D.L., Van Bavel, E., Weidema, F., Leijh, P.C.J. 1987. Ionic channels and membrane hyperpolarization in human macrophages. *J. Membrane Biol.* **97**:251–258
16. Ince, C., Ypey, D.L., Van Furth, R., Verveen, A.A. 1983. Estimation of the membrane potential of cultured macrophages from the fast potential transient upon microelectrode entry. *J. Cell Biol.* **96**:796–801
17. Konijn, T.M., Van de Meene, J.G.C., Bonner, J.T., Barkley, D.S. 1967. The acrasin activity of adenosine-3′,5′-cyclic phosphate. *Proc. Natl. Acad. Sci. USA* **58**:1152–1154
18. Lassen, U.V., Nielsen, A.M.T., Pape, L., Simonsen, L.O. 1971. The membrane potential of Ehrlich ascites tumor cells: Microelectrode measurements and their critical evaluation. *J. Membrane Biol.* **6**:269–288
19. Maeda, M. 1983. Alteration of cellular ionic constituents by external ionic conditions, and its significance in the development of *Dictyostelium discoideum*. *Bot. Mag. (Tokyo)* **96**:193–210
20. Malchow, D., Bohme, R., Gras, U. 1982. On the role of calcium in chemotaxis and oscillations of *Dictyostelium* cells. *Biophys. Struct. Mech.* **9**:131–136
21. Marin, F.T., Rothman, F.G. 1980. Regulation of development in *Dictyostelium discoideum* IV. Effects of ions on the rate of differentiation and cellular response to cyclic AMP. *J. Cell Biol.* **87**:823–827
22. Muller, U., Malchow, D., Hartung, K. 1986. Single ion channels in the slime mold *Dictyostelium discoideum*. *Biochim. Biophys. Acta* **857**:287–290
23. Neumann, E., Gerisch, G., Opatz, K. 1980. Cell fusion induced by electric impulses applied to *Dictyostelium*. *Naturwissenschaften* **67**:414–415
24. Peres, A., Bernardini, G., Negrini, C. 1986. Membrane potential measurements of unfertilized and fertilized *Xenopus*

laevis eggs are affected by damage caused by the electrode. *Exp. Cell Res.* **162:**159–168

25. Persechini, P.M., Araujo, E.G., Oliveira-Castro, G.M. 1981. Electrophysiology of phagocytic membranes: Induction of slow membrane hyperpolarizations in macrophages and macrophage polykaryons by intracellular calcium injection. *J. Membrane Biol.* **61:**81–90
26. Peters, D.J.M., Knecht, D.A., Loomis, W.F., DeLozanne, A., Spudich, J., Van Haastert, P.J.M. 1988. Signal transduction, chemotaxis and cell aggregation in *Dictyostelium discoideum* cells without myosin heavy chain. *Dev. Biol.* **128:**158–163
27. Van Haastert, P.J.M., Konijn, T.M. 1982. Signal transduction in the cellular slime molds. *Mol. Cell. Endocrinol.* **26:**1–17
28. Walsh, J.V., Jr., Singer, J.J. 1980. Penetration-induced hyperpolarization as evidence for Ca^{2+} activation of K^+ conductance in isolated smooth muscle cells. *Am. J. Physiol.* **239:**C182–C189

Received 25 March 1988; revised 1 August 1988

Appendix

For convenience of the reader a summary is given of the mathematical analysis, carried out by Ince et al. [13], of a microelectrode measurement as represented by the electrical equivalent circuit of Fig. 1*B*. We assume that the circuit components are constant during the impalement transient.

At the moment of impalement ($t = 0$), a connection between R_e, R_s, R_m and C_m is made (*as shown in* Fig. 1*B*). Subsequently C_m will discharge from E_m to a new steady-state potential level E_n. If the response time of the microelectrode is sufficiently rapid, the discharge of C_m can be monitored at V_e. At $t = 0$, according to Kirchhoff's laws, the sum of the currents flowing through R_m, C_m, R_s and R_e must be zero. Furthermore, the current through R_e equals the current through C_e (assuming ideal input characteristics of the potential meter V_e). From this, the following relation between the measured potential V_e and the membrane potential E_m is found:

$$T_m T_e \frac{d^2V_e}{dt^2} + (T_m + T_c + \beta T_e)\frac{dV_e}{dt} + \beta V_e = \frac{R_m}{R_s} E_d + E_m \quad (3)$$

in which $T_m = R_m C_m$, $T_e = R_e C_e$, $T_c = R_m C_e$ and $\beta = (R_s + R_m)/R_s$.

In the steady-state condition ($t \to \infty$), Eq. (3) reduces to Eq. (1), where $V_e = E_n$.

Only for measurements where $R_s \gg R_m$ (*e.g.*, in patch-clamp measurements) Eq. (1) reduces to $E_n = E_m$. When R_s is in the order of magnitude of R_m, however, measurement of the peak potential E_p provides a more accurate measure of E_m than does E_n.

Since all coefficients in Eq. (3) are positive, the solution of Eq. (3) will be of the form:

$$V_e = A \exp(Q_1 t) + B \exp(Q_2 t). \quad (4)$$

From the characteristic equation and the initial conditions ($V_e = 0$ and $dV_e/dt = E_m/T_e$ at time $t = 0$) the factors Q_1, Q_2, A and B can be calculated. The factors A, B, Q_1 and Q_2 are respectively:

$$A = (E_m/T_e + Q_2 E_n)/(Q_1 - Q_2) \quad \text{and}$$
$$B = -(E_m/T_e + Q_1 E_n)/(Q_1 - Q_2) \quad (5)$$

$$Q_1, Q_2 = \frac{(T_m + \beta T_e + T_c) \pm [(T_m + \beta T_e + T_c)^2 - 4\beta T_m T_e]^{1/2}}{-2T_m T_e}. \quad (6)$$

From the model and the mathematical description it is clear that E_m cannot be calculated by exponential extrapolation back to the moment of cell penetration of the depolarizing tail of the impalement transient as proposed by Lassen et al. [18]. This is due to the presence of the capacitive load imposed by C_e on the discharge of the membrane.

The value of E_p can be calculated by substitution of Q_1, Q_2, A and B and of t_p (*i.e.*, the time it takes V_e to reach E_p) in Eq. (4) [13]. The value of E_p is given by:

$$E_p = A(-Q_1 A/Q_2 B)^{Q_1/(Q_2 - Q_1)} + B(-Q_1 A/Q_2 B)^{Q_2/(Q_2 - Q_1)} + E_n. \quad (7)$$

A more detailed analysis of the model behavior under various conditions is described by Ince et al. [13].